---

**Article:**
Rasid, A.F.A. and Zhang, Y. orcid.org/0000-0002-9736-5043 (2018) Combustion characteristics and liquid-phase visualisation of single isolated diesel droplet with surface contaminated by soot particles. Proceedings of the Combustion Institute. ISSN 1540-7489

https://doi.org/10.1016/j.proci.2018.08.023

---

# Combustion Characteristics and Liquid-phase Visualisation of Single Isolated Diesel Droplet with Surface Contaminated by Soot Particles

Ahmad Fuad Abdul Rasid[1,a,b,*] and Yang Zhang[2,b]

[1]afabdulrasid1@sheffield.ac.uk, +44(0)7553165442,

[2]yz100@sheffield.ac.uk, +44(0)1142227880

[a]*Fakulti Teknologi Kejuruteraan (FTK), Kampus Teknologi, Universiti Teknikal Malaysia Melaka, Hang Tuah Jaya, 76100 Durian Tunggal, Melaka, Malaysia.*

[b]*Department of Mechanical Engineering, The University of Sheffield, Sir Frederick Mappin Building, Sheffield, S1 3JD, United Kingdom*

**Colloquium**

Spray, Droplet, and Supercritical Combustion – Combustion of droplets

**Total length of paper**

| Figure | Word Count (Method 1) | Sections | Word Count |
|---|---|---|---|
| 1 | 243 | Introduction | 847 |
| 2 | 90 | Experimental Setup | 841 |
| 3 | 129 | Results and Discussions | 1782 |
| 4 | 592 | Conclusions | 334 |
| 5 | 226 | Figures | 1944 |
| 6 | 246 | Equations | N/A |
| 7 | 418 | References | 384.56 |
| **Total** | **1944** | Acknowledgement | 26 |
| | | **Total words** | **6158.56** |

The author confirms to pay colour reproduction charges

**List of Figures**

Fig. 1 Imaging setup and ignition approach on diesel fuel droplet by (a) thermal wire ignition and (b) diesel flame ignition.

Fig. 2 Four typical images of droplet with varying degrees of soot contamination.

Fig. 3 Combustion phases of a diesel

Fig. 4 Droplet squared diameter and flame stand-off ratio regression of (a) thermal wire ignition and (b) diesel flame ignition..

Fig. 5 Quantitative measurement of average burning rate and lifetime of combustion phases on different ignition approaches.

Fig. 6 Sequential soot contamination process of (a) initial condition, (b) agglomeration of soot, (c) agglomerated soot shell formation and (d) formed soot shell at ignition.

Fig. 7 Ignition, swelling, boiling and disruptive phases of diesel droplet ignited by (A) thermal wire ignition; neat and (B) diesel flame ignition; soot contamination.

**Abstract**

The combustion generated soot contamination effect on a single diesel droplet ignition and burning was investigated experimentally for the first time. Diesel droplet flame was used to contaminate the droplet to be investigated prior to ignition. Distinct differences in lifetime and stability of the burning of the neat and contaminated droplet samples were observed in their heating, boiling and disruptive phases. For a soot-contaminated droplet surface, the evaporation rate became weaker as a result of slower mass transfer thus contracted the flame formation. Contrary to the burning rate enhancement of droplet with stable and uniform suspension of particles observed by other researchers, the slightest contamination of soot particles in a fuel droplet surface can significantly reduce the burning rate. Denser agglomeration of soot can form a shell on the droplet surface which blocks the flow of gas escaping through the surface thus distort the droplet even further. At late combustion stage, bubbles are observed to rapture on the surface of the soot-contaminated droplet. Strong ejections of volatile liquid and vapor that would explode shortly after parting from the droplet are observed. It seems that the explosion and burning of ejected mixture have little interactions with the enveloped flame surrounding the primary droplet. Enhanced visualisation of droplet liquid-phase has clearly indicated the cause of declining trend in the burning rate and flame stand-off ratio of soot-contaminated diesel droplet. These insights are of significance for understanding the effect of fuel droplet contamination by combustion generated soot particles.

*Keywords*: Droplet combustion; Soot contamination; Liquid-phase visualisation; Disruptive burning; Combustion Lifetime

## 1.0 Introduction

Particle suspensions are known to have significant effect on fuel droplet combustion. Interestingly, little research is done on combustion generated soot contamination of a droplet, which is going to be investigated in this paper for the first time. Until recently, combustions of fuel droplet with initial uniform particle suspension and high carbon mixture lead to a significant area of study, which mainly examines the effects of particle agglomeration to the burning rate, lifetime and combustion phases. The studied fuel droplet is considered to vaporise either based on the order of volatility with high mass transport inside the droplet, which follows the theory of batch distillation, or with a liquid-phase diffusion theory which implies that the mass transport inside the droplet is slow in relation to the droplet surface regression [1, 2].

In combustion of light diesel oil and heavy oil residue mixtures, Xu et al. [3] observed two distinct combustion phases with different evaporation rate which were volatile liquid-phase evaporation and oxidation of solid soot and coke upon flame extinction. In liquid evaporation phase, the burning rate follows the regression of their volatile component and eventually decreases as it progressed to a solid oxidation phase. Formation of shell of agglomerated particles lead to multiple microexplosions and suppressed the evaporation rate as the liquid-phase evaporation progressed. In smouldering phase of solid particles, soot vaporised quicker than coke with distinct burnout time between them [4]. However, final solid coke did not burn and remained on the suspender [1]. Thick soot and coke formed during combustion divides the regression of steady combustion phase into two distinctive trends because they evaporate by their order of volatilities, similar to batch distillation theory.

Further optimising particle dilution in base fuel, nanofluid concept was established [5]. Javed et. Al [6] conducted a study on various dilute concentrations of aluminium particles in kerosene and heptane droplets combustion concluded that metallized liquid fuel burns with higher

combustion energy due to higher gravimetric energy contents. However, if the ratio of aggregates to the base fuel are high enough, they acted as a heat sink throughout the combustion and eventually lead to flame extinction [7]. Three distinct phases were observed by Takahashi et. al [8] which involved steady combustion, shell formation and microexplosion. As the steady combustion phase progressed, the combustion temperature is controlled by lower volatile component. Higher boiling point of low volatile particle increases the temperature within the surface layer, resulting temperature gradient across the droplet [9] and characterised similar to liquid-phase diffusion theory. In disruptive phase, particles accumulated on the droplet surface formed an impermeable shell and superheat the fuel heterogeneously that lead to microexplosions [10]. Combustion of nanofluid experienced similar disruptive phase and shell formations with various slurry fuel studies [11-12], but with lesser magnitude of disruptions and deviations of linear droplet surface regressions.

There are some studies discussed on the soot formation and fuel droplet contamination during combustion process. Study of jet interaction on cylinder wall by Shaw and Williams [13] suggested that there is a boundary between the diffusion flame and the soot parted from the flame that allowed impingement of soot on the cylinder wall. This suggests the availability of deposited soot to dilute the mixture and possibly the droplet in fuel spray. Kittelson and Kraft [14] discussed that some particles which re-enter the cylinder through exhaust gas recirculation (EGR) can survive the oxidation process upon entering and may act as a sponge and attached to other remaining fuel droplets, engine oil and soot particles. Also, soot typically forms in rich region of combustion chamber which is nucleated from vapor phase to solid phase [15]. The early ignited spray flame may also contaminate the late spray droplets through turbulent mixing process. Possible source of contaminations includes soot build-up inside the cylinder, recirculated exhaust gas and early formation of soot in rich region of fuel spray.

Despite various discussions on the possibility of soot contamination, experimental analysis on combustion behaviour of continuous, random and non-stabilised contamination of soot particles on a fuel droplet surface is not present. In this regard, the aim of this paper is to experimentally examine the combustion characteristics of isolated diesel droplets contaminated with solid soot particles. The surface to volume ratio of a group of fine droplets in a spray is much larger than that of a single droplet having the same mass. Therefore, higher possibility of soot contamination on the droplet surface is expected during actual process than the relative large single droplet burning test. Different from various stable suspension of slurry and nanofluids where the solid particles are evenly distributed inside base fuel, only the base fuel droplet surface was contaminated by the sooty flame released by the neat burning droplet used in this work to ignite the droplet. In this paper, enhanced imaging technique is applied to observe the droplet dynamics with clear view inside the droplet throughout its combustion lifetime. The aim is to visualise the dynamics of soot contamination in a droplet as well as the interaction between combustion and droplet, especially in its liquid-phase at high speed, magnification and clearer view.

## 2.0 Experimental Setup

The fuel used in this experiment was commercial Shell diesel as base fuel. The experimental setup is shown in Fig. 1. For tracking droplet lifetime and droplet dynamics at high speed, a Phantom V210 and a Photron-SA4 high speed colour cameras were used alternately. A backlighting imaging was conducted by placing an IDT 19-LED high intensity illuminator with a diffuser behind the droplet which is opposite to the camera lens (Nikon AF Micro NIKKOR 60mm f/2.8D). Additionally, a direct flame imaging was conducted simultaneously by positioning a Photron-SA4 high speed colour camera with its optical path in perpendicular axis of droplet imaging with Nikon AF Nikkor 50 mm f/1.8D lens attached to it. For droplet liquid-phase imaging, 10000 frames per second with x40

magnification was set. Direct flame imaging was done with 500 frames per second with x5 magnification. Droplets initial diameters were kept constant at 1±0.05 mm for each test and were suspended on 100 µm silicon carbide fibre. The recording of images was between the ignition to the flame extinction of the droplet combustion.

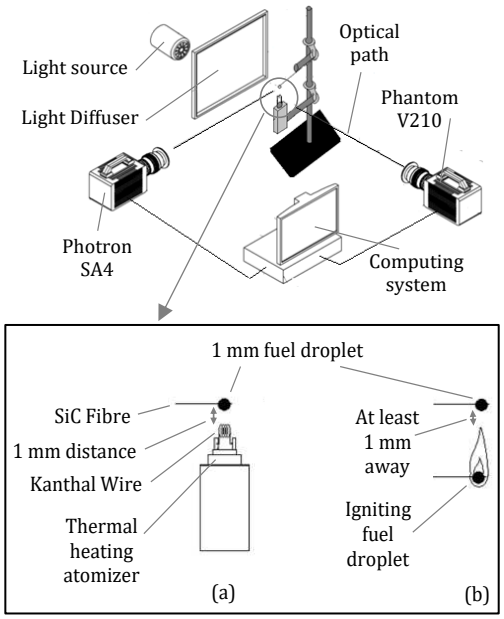


Fig. 1 Imaging setup and ignition approach on diesel fuel droplet by (a) thermal wire ignition and (b) diesel flame ignition.

Two different ignition approaches were applied in this study. The first method can be seen in Fig. 1(a), the droplet was ignited by a thermal heating Kanthal wire positioned 1 mm away from the droplet. The ambient air below the droplet surface was heated by up to 800 ℃ to produce an ignition with zero soot contamination. The thermal wire was removed upon the first appearance of flame formation. The second approach is shown in Fig. 1(b). The diesel droplet was ignited with another diesel droplet and the igniting flame edge was at least 1 mm away from the upper droplet. The lower diesel droplet was ignited by thermal wire to ensure neat combustion of the igniting droplet. Upon the first appearance of flame formation on the upper droplet, the burning lower droplet was removed. The degree of contamination from the combustion of the first droplet is

varied from light to heavy as the images shown in Fig. 2. With random contamination which simulates an actual process specific to laboratory controlled vertical ignition, the effects on combustion characteristics between them were investigated. The removal of the ignition source was done in quick succession in each individual measurement to minimise the uncertainties of measurement during ignition process.

Typical area covered by agglomerated shell of soot in contaminated droplet was approximated to be 79% by measuring the area in MATLAB using segmentation and two-dimensional area measurement functions. Assuming the thickness of agglomerated shell to be 50 nm, minimum soot contamination loading was estimated to be the order of 0.02% by volume.


Fig. 2 Four typical images of droplet with varying degrees of soot contamination.

The codes used to process all the result obtained are segmentations and feature extractions coding developed in MATLAB scripts, which is able to evaluate the dimensions of threshold images via digital image processing tools. Regressions of droplet evolution presented in this paper are based on normalised squared diameter $(D^2/D_o)^2$ against normalised time $t/(D_o)^2$ throughout the droplet combustion; termed $D^2$-law originally proposed by Langmuir [16]. The D and t represent the current sequential droplet diameter and time respectively whilst $D_o$ represents the initial droplet diameter. One regression from processed images was selected to demonstrate the combustion phases in Fig. 3. As shown in the figure, the droplet began to expand and swell upon ignition and denoted as Phase I (swelling). The main characteristic of this phase is a non-linear regression in the squared diameter lifetime of droplet combustion indicating that the droplet continues to expand

while burning at the same time. Zhu et. al [17] discussed that the presence of this curve was due to the droplet swelling that compensates for mass loss, thus not accountable for quasi-steady calculations. Hence, no quantitative measurements of burning rate constant, K were done in this phase. As the expansion of the droplet receded, the squared diameter of the droplet began to linearly reduce. Large size of droplet (1000 µm) together with high vaporisation rates of burning droplet would produce a temperature gradient from the surface to the core of the droplet that varies with time [18]. Because of this reason, slight puffing might occur and mild oscillations of the droplet are observable. Quantitative measurements on the droplet during this phase conforms with $D^2$-law [16], which dictates that squared droplet diameter will decrease linearly with time. This linear regression of burning phase denoted as Phase II (boiling), which is used for the reliable measurement of burning rate constant, K. Higher disruptive regression was observed as the combustion progressed. More viscous droplet surface formed as a result of fuel decomposition [19], mainly caused by the particle agglomeration and denoted Phase III (disruptive). During this phase, measurements of burning rate were not precise as the disruptive behaviour of bubble ruptures did not follow the classical $D^2$-law clearly illustrated in the Fig. 3 and discussed by various researchers [7, 20]. Upon fuel depletion, soot particles were observed to have fully oxidised, which has little difference between both neat and soot contaminated droplet; with negligible effect on fuel decomposition and soot depositions.

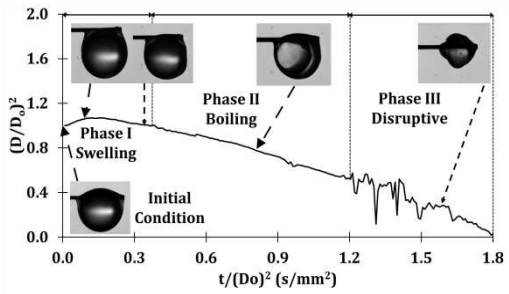


Fig. 3 Combustion phases of a diesel

## 3.0 Results and Discussions

High speed images were captured in each sample at least four times to ensure their repeatability and precision. This section further discusses the regression of droplet squared diameter, flame stand-off ratio, burning rate, lifetime of combustion phases as well as liquid-phase monitoring of burning droplets experimented in this work

### 3.1 Evolution of Droplet and Flame Stand-off Ratio ($D_f/D$)

Fig. 4 shows the repetitive measurements of squared droplet diameter and flame stand-off ratio for both thermal wire in Fig. 4(a) and diesel flame ignition in Fig. 4(b). The flame stand-off ratio is defined as the current sequential flame height, $D_{f,}$ over the droplet diameter, D. Regressions from the figure demonstrated high repeatability of quantitative measurements conducted in this work. Brief measurement uncertainties are shown in the regression of flame stand-off ratio between normalised lifetime of 0.15 to 0.18 s/mm$^2$ in Fig. 4(a) and 0.07 to 0.1 s/mm$^2$ in Fig. 4(b) with slight elevation in flame formation. This is due to the interaction between imaged droplets and their igniting media prior to isolation. Actual imaging periods of neat diesel combustions were between 2040 to 2350 ms and between 1180 to 1500 ms in contaminated diesel droplets in their individual measurements.

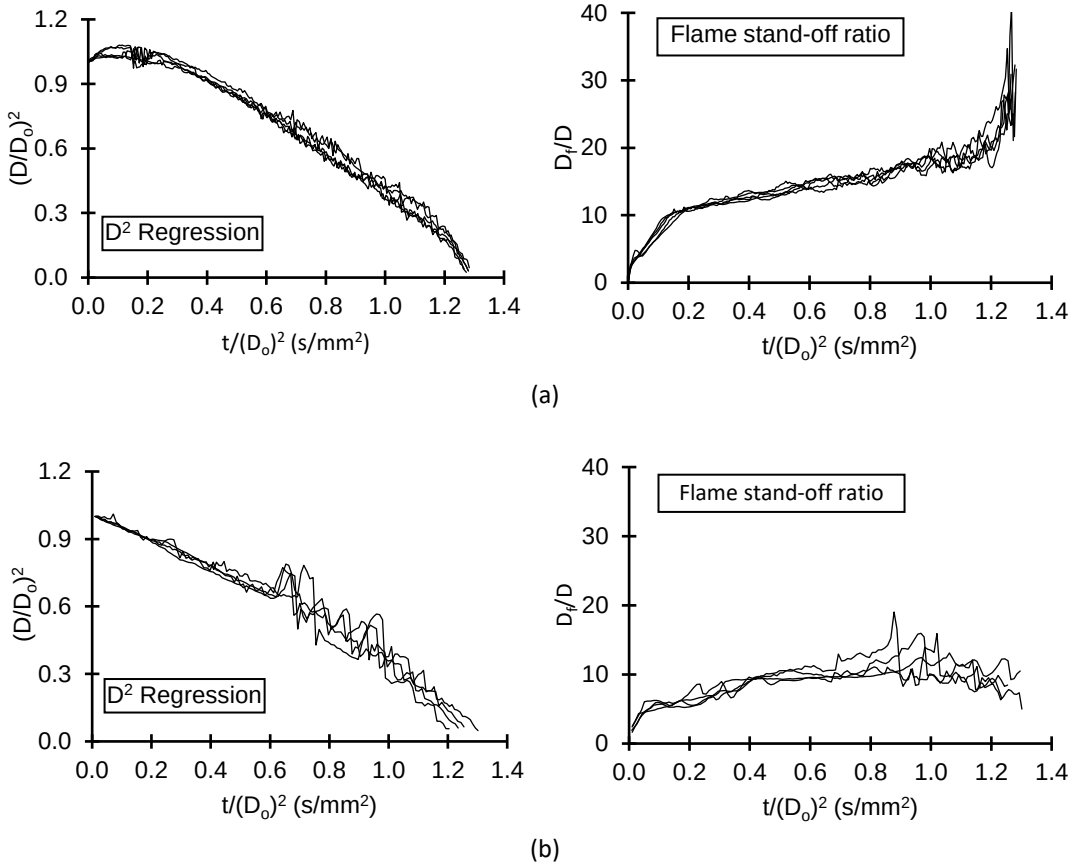


Fig. 4 Droplet squared diameter and flame stand-off ratio regression of (a) thermal wire ignition and (b) diesel flame ignition.

Most work on droplet ignition used low frame rate to image the droplet evolution, between 30 to 5200 fps [1, 7-9] thus making the droplet evolution appeared to have less disruptive behaviour. This work aims to precisely differentiate the effect of soot contamination using a higher frame rate of image capture at 10,000 fps and magnification of x40, which is able to clearly record the disruptive behaviours on the droplet surface during combustion. Soot contamination in diesel flame ignition shortened the total lifetime of the droplet due to its frequent microexplosions and fuel ejections shown by extreme fluctuation in the regression. Lower mass diffusion in contaminated droplet reduced expansion rate of the droplet in Phase I, which is observed to have expanded later at normalised lifetime of 0.4 s/mm$^2$. Early agglomeration of soot reduces distortions of the droplet surface in early combustion process indicating lower amount of gas escaped through

thus stabilised the surface as the droplet core temperature reached its boiling temperature of Phase II at slower rate.

The effect of droplet interaction to the regression of flame stand-off ratio can be determined by synchronised imaging between droplet evolution and flame formation implemented in this work; by evaluating the disruptive pattern between them. Flame stand-off ratio declined as the combustion of contaminated droplet progressed shown in Fig. 4(b). In this case, soot particles promote agglomeration at faster rates which in turn contract the flame formation due to the suppressed evaporation rate. Droplet surface ruptures occurred actively during Phase III, ejecting smaller droplets, vapor and soot agglomeration. Increasing trend of flame stand-off ratio in neat diesel droplet shows high droplet interaction, suggesting multiple interaction between the burning of main droplet and ejected sub droplets. However, trend of flame stand-off ratio of contaminated droplet shows otherwise despite of having higher occurrence of bubble ruptures. Hence, there is the need for clear visualisation of the dynamics inside the droplet to identify such a significant difference, which is discussed in the liquid-phase monitoring section.

### 3.2 Average Burning Rate Constant

Despite of recorded disruptive regression on the lifetime of squared droplet diameter, both case in Fig. 4(a) and (b) still follows the classical theory of $D^2$-law in Phase II. Measurement of burning rate shown in Fig. 5 indicates even the slightest contamination of soot particles has reduced the burning rate of neat diesel significantly by at least 17%. The early agglomeration of soot shells formed on the surface of the droplet reduces the liquid diffusion of fuel from the interior to the surface which in turn suppresses the evaporation process. The superheated liquid within the shell will promote multiple gas nucleation that would break free through the shell thus lead to enhanced disruption. Denser contamination by diesel flame ignition does not have significant further reduction to the

measured burning rate as shown by the very small deviation between each measurement in Fig. 5 but with more profound magnitude of disruptive behaviours clearly shown in Fig. 4(b). Large differences in combustion characteristic were observed between stable dilution of nanoparticles and soot contaminated droplet. Small amount of stabilised particle loadings improves the burning rate [6-7] whereas even the slightest contamination of soot significantly reduces the burning rate.

### 3.3 Lifetime of Combustion Phases

Imaging techniques applied in this work made the identification of each combustion phases possible by their distinct changes from one phase to another in thermal wire and diesel flame ignition. Soot contamination prior to ignition deviated the regression from $D^2$-law longer in the quantitative measurement of the lifetime in Phase I and Phase III shown in Fig. 5. Diesel flame ignition recorded to have the shortest reliable measurement of burning rate in Phase II with only 58% of its total lifetime. Soot deposited on the surface of the droplet was found to reduce the liquid diffusion from the core to the surface of the droplet throughout the combustion and it obstructs the nucleated gas to escape through the droplet surface during the combustion process. This in turn prolonged the lifetime of Phase I and III. In addition, soot agglomeration was observed to promote high disruptive effect by nucleating inside the droplet heterogeneously, diminishing the stability of steady combustion and transitioned the combustion to Phase III earlier. Contaminated droplet combustion is found to have longer disruptive phase with 12.7% of its total lifetime.

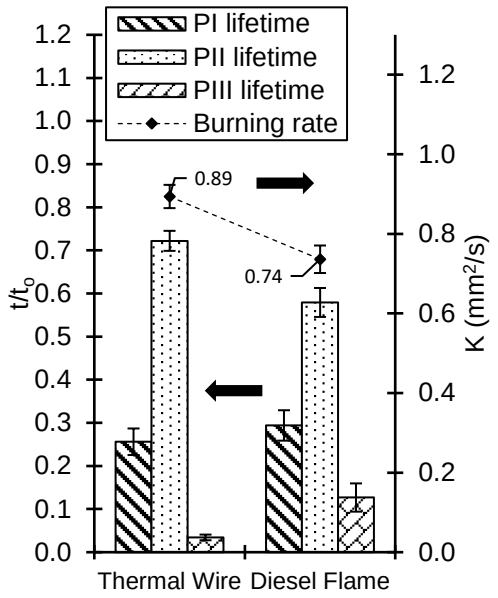


Fig. 5 Quantitative measurement of average burning rate and lifetime of combustion phases on different ignition approaches.

Denser soot contamination is found to increase the magnitude of disruptive behaviour of the droplet surface due to the thickened soot shell. Nucleated gas trapped inside the droplet would require higher pressures to be released through the thicker soot shell thus further disoriented the droplet surface. Flame formations are observed to fluctuate in relation to the degree of droplet disruptive behaviours. However, the variation of soot contamination degrees on the surface of the droplet is found to have very small influence on the duration of lifetimes in each combustion phase. Deviations in length of lifetime in each phase shown in Fig. 5 for contaminated droplet were less than 4%. Typical findings on stable and uniformly suspended particle suggests earlier and longer period of disruptive combustion with higher concentration of precursors and nanoparticles [6-7, 9-10]. Those findings, however, are distinctly different from the random soot contamination on a droplet surface because they are not in the same particle laden condition as the present work.

3.4 Liquid-Phase Visualisation

Unique approach in droplet combustion characteristics study was conducted by an actual visualisation on the dynamics of soot contamination on the droplet surface as well as clear view inside the droplet during combustion process. Different from droplet combustion imaging done by others [1, 6-10], unique insight on the relation between the combustion behaviour and the dynamics of the droplet in liquid-phase is gained. Prior to ignition, soot particles released by the hot gas from the lower positioned diesel droplet flame were quenched as soon as they contacted the droplet surface. As a result, a thin layer of agglomerated soot particles immediately formed on the surface of the droplet shown in Fig. 6. This process is the primary mechanism of soot contamination on the small fuel droplet, specific to laboratory controlled vertical ignition with different contamination densities.

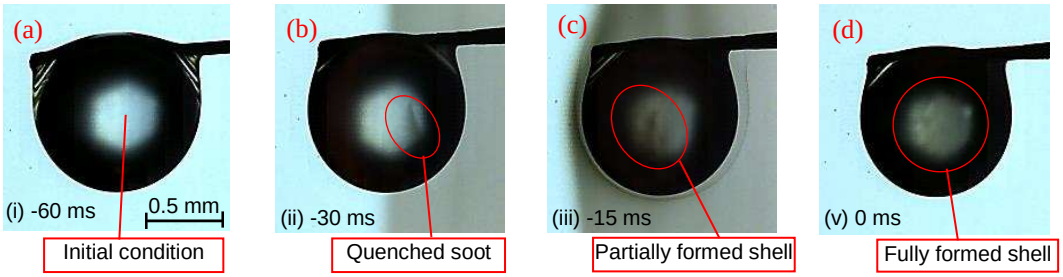


Fig. 6 Sequential soot contamination process of (a) initial condition, (b) agglomeration of soot, (c) agglomerated soot shell formation and (d) formed soot shell at ignition.

In Phase I, the surface of neat droplet moderately distorted and depicted in Fig. 7(A, ii). This indicates the presence of temperature gradient across the droplet. Throughout this process, several spots that reached the boiling temperature in the droplet nucleated the gas locally, releasing vapor that escaped through the surface and distorted the droplet surface through continuous occurrences. Very little distortion shown by diesel flame ignition in Phase I due to a reduced liquid and gas diffusion caused by the shell that formed immediately upon ignition. As Phase II

combustion progressed in diesel flame ignition, denser agglomeration of soot shell further obstructed escaping fuel vapor. As a result, higher vapor pressure distorted the surface even more and able to eject with some of the agglomerated soot particles as it puffed shown in Fig. 7(B, ii).

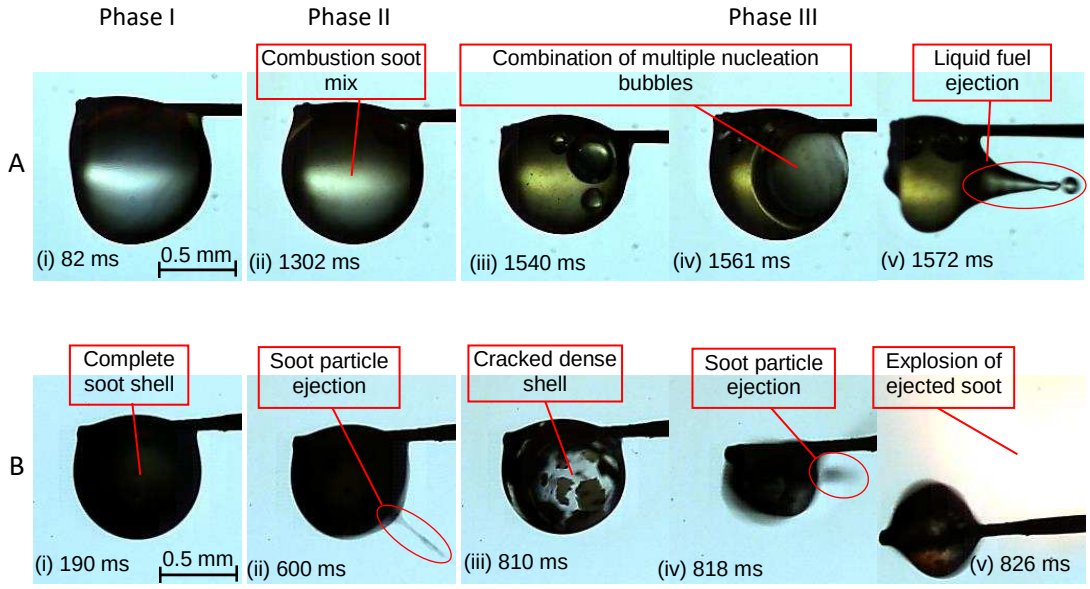


Fig. 7 Ignition, swelling, boiling and disruptive phases of diesel droplet ignited by (A) thermal wire ignition; neat and (B) diesel flame ignition; soot contamination.

As the combustion transitioned into Phase III, nucleation sites began to actively appear within the droplet, shown in Fig. 7(A, iii) of neat diesel. In this phase, the fuel viscosity further increased due to the decomposition of fuel [19]. Because of these reason, bubbles of nucleation site have the tendency to be combined rather than escaping through the surface shown in Fig. 7 (A, iv). As a result, higher pressure of escaped vapor pushed the viscous liquid and appeared as liquid fuel ejection shown in Fig 6(A, v). Ejected sub-droplets burned shortly after parting, further intensify the flame formation of both primary and ejected sub-droplet thus elevated the regression of flame stand-off ratio in Fig.4(a) in later stage of combustion. Simultaneous burning of nearby sub-droplets forms larger enveloped flame indicating the characteristics of interacting droplet combustion [20]. Similar behaviours were observed in repetitive measurements on neat diesel droplet and it was found that the interacting combustion between primary and ejected sub-

droplets is the main cause of increasing trend in the regression of flame stand-off ratio towards flame extinction.

In the case of soot contaminated droplet, soot shell formed prior to ignition was not fully oxidised and fragmented during the combustion process. At least 60% of total droplet area was covered by the fragmented shell with darker appearance because of the thickened soot shell shown in Fig. 7(B, iii). This created a tougher obstruction for the nucleated gas to be released and higher vapor pressure pushed out fragment of the shell together with a burst of volatile diesel vapor shown in Fig. 7(B, iv). Flame from the primary droplet ignited the released vapor thus initiated an explosion outside the droplet shown in Fig. 7(B, v). The explosion interacted with the flame formation of the main droplet, further fluctuating the flame stand-off ratio in Phase III. However, there is no combined enveloped flame created between the primary and ejected droplets. Similar occurrences of vapour ejection with soot particles and non-interacting flame formation were observed in each repetitive visualisation. As the combustion progressed, the probability of sub-droplet shootings is increased. It was observed that the explosion of ejected sub-droplets does not intensify the flame formation of the primary droplet. For this reason, the regression of flame stand-off ratio continued to decline towards flame extinction shown in Fig. 4(b). Distinct differences in combustion interaction of secondary atomisation between neat and soot contaminated diesel droplet was observed by clear visualisation of the dynamics inside the droplet. This demonstrated the importance of enhanced liquid-phase monitoring conducted in this work.

## 4.0 Conclusions

The effects of soot particle contamination in diesel-based fuel droplets have been investigated. Contamination of soot particle on the droplet surface was found to have significantly reduced the

burning rate and promoted disruptive behaviour throughout the droplet lifetime. The results from this study are summarised as follows:

1. Enhanced visualisation of droplet liquid-phase clearly shows the cause of declining trend in the burning rate and flame stand-off ratio of soot contaminated diesel droplet. Dynamics of surface distortion, puffing as well as microexplosions were fully observed and explained.
2. On contact with the surface of the fuel droplet, the soot particles contained in hot combustion gas were quenched and immediately formed solid soot particles that agglomerated to a soot shell on the droplet surface. This process is the primary mechanism of soot contamination in small fuel droplet tests specific to laboratory controlled vertical ignition.
3. Soot contamination reduced the burning rate of neat diesel droplet by 17% and lifetime of steady burning phase by 14%. Higher degrees of soot contamination on the surface of the droplet increased the magnitude of disruptive behaviour on surface distortion and flame formation but has insignificant effects on the lifetime period of individual combustion phases.
4. The envelop flame formed by the ejected liquid fuel will interact with that of the primary droplet during the disruptive phase in the case of thermal wire ignition. This induces high primary droplet and sub-droplets interaction which further intensifies the flame formation and evaporation rate. The more violent explosions of the ejected soot contaminated volatile vapor in the case of diesel flame ignition suppressed the growth of the flame stand-off ratio due to very little flame interactions.
5. Estimated a low 0.02% loadings of soot particles contamination in diesel droplet would reduce the overall evaporation rate as observed in this study. Shell of agglomerated soot formed on the surface layer of the droplet changed the surface tension and at the same time lower the mass transfer during combustion, further suppressing the evaporation rate.

**Acknowledgments**

The authors would like to thank Universiti Teknikal Malaysia Melaka for the Fellowship Scheme and the Ministry of Higher Education Malaysia for SLAB Scholarship Scheme

**References**

[1] M. Ikegami, G. Xu, K. Ikeda, S. Honma, H. Nagaishi, D.L. Dietrich, Y. Takeshita, Fuel 82 (2003) 293–304.
[2] C.K Law, Alche. J. 24 (1978) 626–632.
[3] G. Xu , M. Ikegami , S. Honma , K. Ikeda , H. Nagaishi, Y. Takeshita, Combust. Sci. Tech. 174 (2002) 115-145.
[4] G. Xu , M. Ikegami , S. Honma , K. Ikeda , X. Ma, H. Nagaishi, Combust. Sci. Tech. 175 (2003) 1-26.
[5] S.U.S Choi, ASME Int Mech Eng Congress Expo, San Francisco, CA, 1995, 99–106.
[6] I. Javed, S.W. Baek, K. Waheed, Combust. Flame 162 (2015) 774–787.
[7] M. Ghamari, A. Ratner, Fuel 188 (2017) 182–189.
[8] F. Takahashi, F.L. Dryer, F.A. Williams, Symp. (Int.) Combust. 21 (1986) 1983–1991.
[9] C.D. Rosebrock, N. Riefler, T. Wriedt, L. Madler, S. D. Tse, AIChE J. 59 (2013) 4553–4566.
[10] H. Li, C.D. Rosebrock, N. Riefler, T. Wriedt, L. Mädler, Proc. Combust. Inst. 36 (2017) 1011–1018.
[11] P. Antaki, F.A. Williams, Combust. Flame 67 (1987) 1-8.
[12] S.C. Wong, A.C. Lin, C.E. Wu, Combust. Flame 96 (1994) 304-310.
[13] B. D. Shaw, F. A. Williams, int. j. heat mass transf. 2 (1990) 301-317.
[14] D. Kittelson, M. Kraft, Cambridge Centre for Computational Chemical Engineering (2014) ISSN 1473 – 4273, 2014.
[15] D. K. Srivastava, A. K. Agarwal, T. Gupta, Aero. Air Qua. Res. 11 (2011) 915–920.
[16] I. Langmuir, Phys. Rev. 12 (5) (1918) 368– 370.
[17] M. Zhu, Y. Ma, D. Zhang, Proc. Combust. Inst. 34 (2013) 1537–1544.
[18] C. K. Law, W. A. Sirignano, Combust. Flame 28 (1977) 175-186.
[19] C.H. Wang, K.L. Pan, W.C. Huang, H.C. Wen, J.Y. Yang, C.K. Law, Exp. Therm. Fluid Sci. 32 (2008) 1049–1058.
[20] H. Oyagi, H. Shigeno, M. Mikami, N. Kojima, Combust. Flame 156 (2009) 763–770.